

# Second RPA calculations with the Skyrme and Gogny interactions<sup>\*</sup>

Danilo Gambacurta<sup>1,a</sup> and Marcella Grasso<sup>2</sup>

<sup>1</sup> Extreme Light Infrastructure - Nuclear Physics (ELI-NP), Horia Hulubei National Institute for Physics and Nuclear Engineering, 30 Reactorului Street, RO-077125 Măgurele, Jud. Ilfov, Romania

<sup>2</sup> Institut de Physique Nucléaire, Université Paris-Sud, IN2P3-CNRS, F-91406 Orsay Cedex, France

Received: 27 April 2016 / Revised: 16 June 2016

Published online: 21 July 2016 – © Società Italiana di Fisica / Springer-Verlag 2016

Communicated by N. Alamanos

**Abstract.** The Second Random Phase Approximation (SRPA) is a natural extension of RPA where more general excitation operators are introduced. These operators contain, in addition to the one particle-one hole configurations already considered in RPA, also two particle-two hole excitations. Only in the last years, large-scale SRPA calculations have been performed, showing the merits and limits of this approach. In the first part of this paper, we present an overview of recent applications of the SRPA based on the Skyrme and Gogny interactions. Giant resonances in <sup>16</sup>O will be studied and their properties discussed by using different models. In particular, we will present the first applications of the SRPA model with the finite-range Gogny interaction, discussing the advantages and drawbacks of using such an interaction in this type of calculations. After that, some more recent results, obtained by using a subtraction procedure to overcome double-counting in the SRPA, will be discussed. We will show that this procedure leads to results that are weakly cutoff dependent and that a strong reduction of the SRPA downwards shift with respect to the RPA spectra is found. Moreover, applying this procedure for the first time in the Gogny-SRPA framework, we will show that this method is able to reduce the anomalous shift found in previous calculations and related to some proton-neutron matrix elements of the residual interaction.

## 1 Introduction

Collective modes are a common feature of many-body systems. Typical examples are giant resonances in atomic nuclei [1, 2]. The random-phase approximation (RPA) is a very successful microscopic theory for the study of the main properties of collective states [3]. In RPA, collective excitations are described as superpositions of 1 particle-1 hole (*1ph*) and 1 hole-1 particle (*1hp*) configurations. This method, especially when applied within the Energy Density Functional (EDF) framework, allows to describe fairly good global properties of giant resonances, such as the centroid energy and the total strength distribution. Among its merits, we mention that the RPA preserves the energy-weighted sum rules (EWSR), in the sense of the Thouless theorem [4]. This feature is very important because it guarantees that spurious states associated with broken symmetries are exactly separated in RPA from the physical states of the system.

<sup>\*</sup> Contribution to the Topical Issue “Finite range effective interactions and associated many-body methods - A tribute to Daniel Gogny” edited by Nicolas Alamanos, Marc Dupuis, Nathalie Pillet.

<sup>a</sup> e-mail: danilo.gambacurta@eli-np.ro

On the other hand, the RPA model has some limits. Among them we recall that, by construction, it predicts a perfectly harmonic spectrum and, moreover, the width of the excited states cannot be reproduced except for the single-particle Landau damping and for the escape width (if continuum states are taken into account). A well-known extension of the RPA scheme is the second RPA (SRPA) model which amounts to enlarge the space of basic elementary excitations by including 2 particle-2 hole (*2ph*) configurations and by coupling them with the *1ph* ones and among themselves. This leads to a richer treatment of the excitation modes. The spreading width can be better described because of the coupling with the *2ph* configurations.

However, due to the numerical effort required, SRPA calculations have been performed only recently without resorting to strong simplifications, in the adopted model spaces or in the evaluation of the SRPA matrices. The last few years have seen large-scale SRPA calculations done without resorting to such approximations [5–10]. Performing such calculations makes it possible to identify some specific features of the SRPA model not appearing in previous strongly truncated and simplified calculations. Unexpectedly, the SRPA spectrum is systematically lowered

by several MeV with respect to that obtained in the ordinary RPA, often spoiling the good agreement with data. The origin of this strong shift was unclear until recently and is related to the implicit inclusion of correlations in ground state. Within EDF approaches when beyond mean-field effects are included, this inclusion can lead to double-counting issues [11, 12]. Moreover, some problematic aspects inherent to the SRPA have been recently analyzed and understood as related to the replacement of the correlated ground state with the Hartree-Fock (HF) one, that is generated by the use of the quasi-boson approximation (QBA). This replacement produces a violation of the stability condition at the SRPA level [13]. In deriving the equations of motion in SRPA use is made, as in RPA, of the QBA and it has been argued [14–16] that this approximation is even more severe in SRPA than in RPA. A careful analysis of the merits and limits of the SRPA was presented in ref. [13]. In particular, the violation of the stability condition in SRPA [17] is illustrated and a generalization of the Thouless theorem [4] is proven in the case where a correlated ground state is used. Recently, an approximate and simplified way, with respect to the full SRPA, has been proposed [18], where RPA phonons are used as building blocks to construct the excited states in a multi-phonon picture. This method, although including two particle-two hole configurations in the description of excited states, provides an alternative method to reduce the effect of the strong shift found in SRPA calculations.

In ref. [19], a procedure to avoid double-counting, called the “subtraction” method, as been proposed and applied in several beyond mean-field calculations, see for example refs. [11, 20, 21]. Very recently [12], the subtraction procedure has been applied for the first time within the Skyrme-SRPA framework showing that a considerable reduction of the SRPA downwards shift with respect to the RPA is found.

In this paper, we first show and discuss some SRPA studies performed both with the Skyrme [22, 23] and the Gogny [24] interactions. Then the “subtraction” method will be briefly introduced and some applications presented. In particular, we will show the first applications of the subtraction procedure in Gogny-SRPA calculations, confirming the good results found in the Skyrme case.

The paper is organized as follows. In sect. 2 a brief summary of the formal aspects of the SRPA model is done. In sect. 3 we show the monopole and quadrupole strength distributions in  $^{16}\text{O}$  obtained in RPA and SRPA, employing both the Skyrme and Gogny interactions. In sect. 4 the subtraction procedure is presented and applied. Finally, we draw some conclusions in sect. 5.

## 2 The SRPA scheme

In this section, we briefly discuss the RPA and SRPA framework by following the equations of motion method [3].

Let  $|0\rangle$  be the ground state of the system and  $|\nu\rangle$  its excited states whose energies are  $E_0$  and  $E_\nu$ , respectively.

Let us now introduce the operators  $Q_\nu^\dagger$  in such a way that

$$Q_\nu^\dagger|0\rangle = |\nu\rangle, \quad (1)$$

$$Q_\nu|0\rangle = 0. \quad (2)$$

It can be shown that the following equations hold for an arbitrary operator  $\delta Q$

$$\langle 0|[\delta Q, [H, Q_\nu^\dagger]]|0\rangle = \omega_\nu \langle 0|[\delta Q, Q_\nu^\dagger]|0\rangle, \quad (3)$$

where  $\omega_\nu = E_\nu - E_0$  are the excitation energies.

Let  $|HF\rangle$  be the HF ground state of the system where the hole states below the Fermi energy are filled and the particle states above are empty. In the following, we use the indices  $m, n, p, q$  and  $i, j, k, l$  to indicate, respectively, particle and hole states. In the RPA scheme the  $Q_\nu^\dagger$  operators are assumed to be a linear superposition of one particle-one hole ( $1ph$ ) operators, that is

$$Q_\nu^\dagger = \sum_{pi} X_{pi}^\nu a_p^\dagger a_i - \sum_{pi} Y_{pi}^\nu a_i^\dagger a_p, \quad (4)$$

where for notation simplicity, the coupling to total quantum numbers is not indicated. By inserting the above expression in eq. (3) with  $\delta Q \in \{a_p^\dagger a_i, a_i^\dagger a_p\}$  we obtain

$$\begin{pmatrix} A & B \\ -B^* & -A^* \end{pmatrix} \begin{pmatrix} X^\nu \\ Y^\nu \end{pmatrix} = \omega_\nu \begin{pmatrix} X^\nu \\ Y^\nu \end{pmatrix}, \quad (5)$$

where the RPA matrices are

$$A_{pi,qj} = \langle HF|[a_i^\dagger a_p, [H, a_q^\dagger a_j]]|HF\rangle, \quad (6)$$

$$B_{pi,qj} = -\langle HF|[a_i^\dagger a_p, [H, a_j^\dagger a_q]]|HF\rangle. \quad (7)$$

We stress that the exact ground state  $|0\rangle$  has been replaced by the HF ground state  $|HF\rangle$  in the expressions of the RPA matrices (6), (7). This replacement, also known as QBA, introduces a visible inconsistency since, on the one hand, the definition of the ground state  $|0\rangle$  as the vacuum of the  $Q$  operators is used to derive the formal equations of the motion (3), while, on the other hand,  $|HF\rangle$  is used instead in calculating the expectation values appearing in those equations. Furthermore, the QBA introduces a violation of the Pauli principle since some terms of the double-commutators appearing in the equations of motion are missing.

In the SRPA framework, the  $Q_\nu^\dagger$  operators have a more general expression, containing also  $2ph$  terms

$$\begin{aligned} Q_\nu^\dagger = & \sum_{pi} \left( X_{pi}^\nu a_p^\dagger a_i - Y_{pi}^\nu a_i^\dagger a_p \right) \\ & + \sum_{p<m,i<j} \left( X_{pimj}^\nu a_p^\dagger a_i a_m^\dagger a_j - Y_{pimj}^\nu a_i^\dagger a_p a_j^\dagger a_m \right). \end{aligned} \quad (8)$$

In this case we obtain that the  $X$ 's and  $Y$ 's are solutions of the equations

$$\begin{pmatrix} \mathcal{A} & \mathcal{B} \\ -\mathcal{B}^* & -\mathcal{A}^* \end{pmatrix} \begin{pmatrix} \mathcal{X}^\nu \\ \mathcal{Y}^\nu \end{pmatrix} = \omega_\nu \begin{pmatrix} \mathcal{X}^\nu \\ \mathcal{Y}^\nu \end{pmatrix}, \quad (9)$$

where

$$\mathcal{A} = \begin{pmatrix} A_{mi,pk} & A_{mi,pqkl} \\ A_{pqkl,mi} & A_{mnij,pqkl} \end{pmatrix},$$

$$\mathcal{B} = \begin{pmatrix} B_{mi,pk} & B_{mi,pqkl} \\ B_{pqkl,mi} & B_{mnij,pqkl} \end{pmatrix},$$

and

$$\mathcal{X}^\nu = \begin{pmatrix} X_{mi}^\nu \\ X_{mnij}^\nu \end{pmatrix}, \quad \mathcal{Y}^\nu = \begin{pmatrix} Y_{mi}^\nu \\ Y_{mnij}^\nu \end{pmatrix}.$$

The elements  $A_{mi,pk}$  and  $B_{mi,pk}$  of  $\mathcal{A}$  and  $\mathcal{B}$  are equal to those defined in eqs. (6) and (7) while the others are

$$A_{mi,pqkl} = \langle HF | [a_i^\dagger a_m, [H, a_p^\dagger a_q^\dagger a_l a_k]] | HF \rangle, \quad (10)$$

$$A_{pqkl,mi} = A_{mi,pqkl}^*, \quad (11)$$

$$A_{mnij,pqkl} = \langle HF | [a_i^\dagger a_j^\dagger a_n a_m, [H, a_p^\dagger a_q^\dagger a_l a_k]] | HF \rangle, \quad (12)$$

$$B_{mi,pqkl} = -\langle HF | [a_i^\dagger a_m, [H, a_k^\dagger a_l^\dagger a_q a_p]] | HF \rangle, \quad (13)$$

$$B_{pqkl,mi} = B_{mi,pqkl}^*, \quad (14)$$

$$B_{mnij,pqkl} = -\langle HF | [a_i^\dagger a_j^\dagger a_n a_m, [H, a_k^\dagger a_l^\dagger a_q a_p]] | HF \rangle. \quad (15)$$

Therefore, in SRPA, the QBA is still used. As a consequence of the use of the  $|HF\rangle$  state in the evaluation of the SRPA matrices we obtain, in particular [25, 26]

$$B_{mi,pqkl} = B_{pqkl,mi} = B_{mnij,pqkl} = 0. \quad (16)$$

However, when density-dependent interactions are employed, rearrangement terms appear also in the  $B_{12}$ ,  $B_{21}$ , as shown in ref. [8].

The matrix (10) describes the coupling of  $1ph$  states to  $2ph$  states, while matrix (12) takes into account the coupling between  $2ph$  states themselves. The dimension of these matrices, especially of the latter, can be very large. If we neglect the residual interaction among the  $2ph$  states, the matrix (12) acquires a simple form,

$$A_{mnij,pqkl} = \mathcal{U}(ij)\mathcal{U}(mn)\delta_{ik}\delta_{jl}\delta_{mp}\delta_{nq}(\epsilon_m + \epsilon_n - \epsilon_i - \epsilon_j), \quad (17)$$

where  $\mathcal{U}(ij)$  is the antisymmetrizer for the indices  $i, j$  and the  $\epsilon$  quantities are the HF single particle energies. In this case, the SRPA problem can be reduced to an RPA eigenvalue problem (5), (whose dimensions are determined by the  $1ph$  space), but where the matrix (6) depends now on the excitation energies  $\omega$  [26].

As mentioned above, many SRPA applications have been indeed performed by using very small model spaces for the  $2ph$  sector and by making use of the so-called ‘‘diagonal’’ approximation (17). Only recently, full SRPA calculations have been carried out, showing that in some cases this approximation is not justified [7, 9].

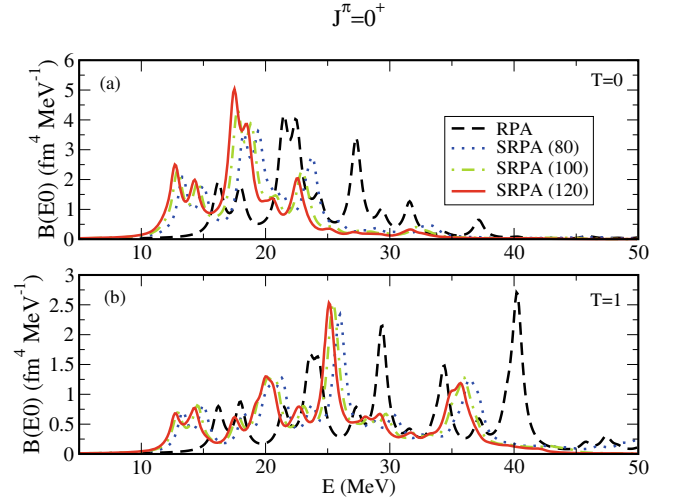


**Fig. 1.** (Color online) Monopole strength distributions in the isoscalar (upper panel) and isovector (lower panel) channels obtained in Skyrme-SRPA for increasing values of the energy cutoff, indicated in MeV in parenthesis in the figure, on the  $2ph$  configurations.

## 3 Results in $^{16}\text{O}$

### 3.1 The Skyrme-SRPA case

In this section we present the nuclear strength distributions in  $^{16}\text{O}$  obtained in Skyrme-SRPA for the monopole and quadrupole multipolarities and we compare them with the RPA ones. The SGII [27] parametrization of the effective interaction is used in the present calculations.

In order to make simpler the comparison between different results, we have folded the discrete spectra coming out from our calculations with a Lorentzian with a width of 1 MeV. The continuous strength distributions shown in this work are thus obtained by using this smoothing procedure.

In RPA calculations,  $1ph$  configurations with unperturbed energy up to 100 MeV are considered, while in the SRPA ones, we have considered all the  $2ph$  configurations with an unperturbed energy lower than an energy cutoff  $E_{cut}$ . In figs. 1 and 2 we show the monopole and quadrupole strength distributions, respectively, for different choices of  $E_{cut}$  (indicated in MeV in parenthesis in the figures). From the figures we see that a cutoff equal to 120 MeV gives stable results. Similar stability checks have been systematically made for all the results shown in the following.

The multipole transition operators used are

$$F_\lambda^{IS} = \sum r_i^2 Y_{\lambda 0}(\hat{r}_i), \quad (18)$$

$$F_\lambda^{IV} = \sum r_i^2 Y_{\lambda 0}(\hat{r}_i) \tau_z(i), \quad (19)$$

in the isoscalar and isovector channel, respectively.

In both isoscalar and isovector cases the strongest effect in SRPA is a several-MeV shift of the strength distribution to lower energies with respect to RPA. This result

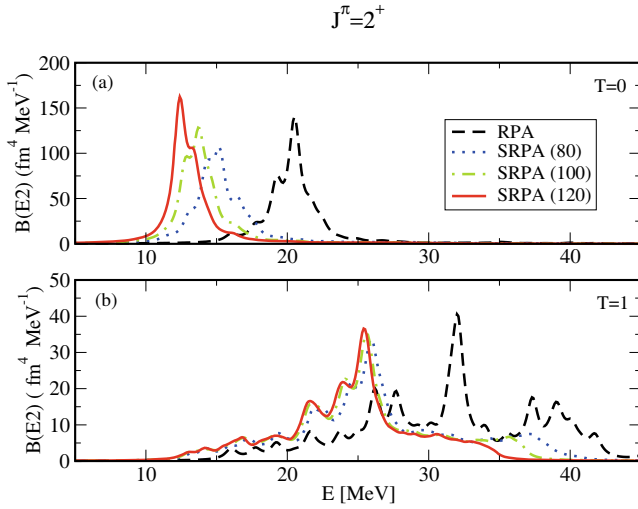


**Fig. 2.** (Color online) Quadrupole strength distributions in the isoscalar (upper panel) and isovector (lower panel) channels obtained in Skyrme-SRPA for increasing values of the energy cutoff, indicated in MeV in parenthesis in the figure, on the  $2ph$  configurations.

seems to be a general feature of SRPA and has been found also in different SRPA calculations [5,6,28]. Looking at the figures, however, one sees that the profiles of the strength distributions are not very much changed, except for the above-mentioned shift.

### 3.2 The Gogny-SRPA case

In the following we will show some Gogny-SRPA calculations. Although the use of a finite-range interaction turns out to be numerically more demanding with respect to the zero-range case, it presents some advantages. The first one is related to the fact that the Gogny force has been introduced and adjusted to be used in both the HF and the pairing channels. Since in the SRPA framework not only the standard RPA-type particle-hole ( $ph$ ) matrix elements of the interaction are present, it seems to us that the use of a force tailored to handle also other kinds of terms, such as the particle-particle matrix elements, is more appropriate. A second, non-negligible, advantage is the finite range of the four central terms of the Gogny force. We expect that this feature provides, in a natural way, convergent results with respect to the increase of the energy cutoff in the  $2ph$  space of the SRPA calculations. At the same time we recall that, in the present calculations the density-dependent zero-range type term is included in the interaction.

We will focus our attention to the monopole isoscalar response. The calculations are performed in spherical symmetry in the harmonic-oscillator basis and the D1S parametrization is used [29, 30]. All the single-particle states with an unperturbed energy lower than 60 MeV (that is, all the  $1ph$  configurations with an unperturbed excitation energy up to 100 MeV) are included in the calculations. This choice ensures that the values of the

energy-weighted sum rules (EWSR) are stable. As previously done, in order to study the stability of the SRPA results against the  $2ph$  configurations, we have considered all the configurations with an unperturbed energy lower than an energy cutoff  $E_{cut}$  and progressively increase it. This kind of study has allowed to single out a problematic behavior of the SRPA results in the Gogny case. We have found that in the Gogny-SRPA model some neutron-proton ( $\nu\pi$ ) matrix elements of the interaction, appearing in the beyond-RPA block matrices, are rather large, some of them being from 5 to 10 times larger than all the other (typical) matrix elements. These matrix elements, not appearing in standard RPA calculations, have a strong impact on the stability of the results, in particular on the peak structure of the response. It has been found that their effects are especially strong in the matrix elements coupling  $1ph$  and  $2ph$  configurations. We have thus performed two different kinds of calculations in order to analyze and single out the effects of these matrix elements. We have considered a) a full SRPA calculation where all the  $2ph$  configurations are included; b) a calculation performed by considering only the  $2ph$  configurations that are composed by pure neutron or proton excitations. This means that in the case b) we do not include the  $2ph$  configurations where the two particles and the two holes have a different isospin nature. As a consequence, no  $\nu\pi$  matrix elements of the interaction are present in the SRPA matrices in the case b). The  $\nu\pi$  matrix elements would appear i) in the case where the  $2ph$  configurations were composed by 1 pure neutron and 1 pure proton  $1ph$  configurations (standard RPA  $1ph$  configurations); ii) in the case where both  $1ph$  configurations were  $\nu\pi$   $1ph$  configurations (typical charge-exchange  $1ph$  configurations). In the case of the  $A_{1ph,2ph}$  matrix we have checked that the majority of the matrix elements are relatively small (of the order of 0.2–0.7 MeV), the mean value being 0.2 MeV. However, some  $A_{1ph,2ph}$  matrix elements are much larger (up to 10 times) and, in particular, the largest ones are due to the presence of 3 hole-1 particle  $\nu\pi$  matrix elements of the residual interaction of the type:

$$\langle \nu^{-1}\pi | V | \nu^{-1}\pi^{-1} \rangle_A, \quad (20)$$

$$\langle \pi^{-1}\nu | V | \nu^{-1}\pi^{-1} \rangle_A, \quad (21)$$

where “A” stands for “Antisymmetrized”. The angular momentum coupling is done between the first-third and second-fourth indices. In the largest  $A_{1ph,2ph}$  terms the strongest contributions are matrix elements of the residual interaction of the type (21) (charge-exchange type). We stress that also some 3 hole-1 particle matrix elements of the residual interaction involving only neutron or proton states are larger than the typical ones. However, they are few and we checked numerically that the strong changes in the SRPA response are not related to them. In the approximation b), also the  $\nu\pi$  matrix elements of the matrix  $A_{2ph,2ph}$  (the matrix that couples among themselves the  $2ph$  configurations) are neglected. However, these matrix elements are not expected to have a strong impact and this will be shown later in this work.

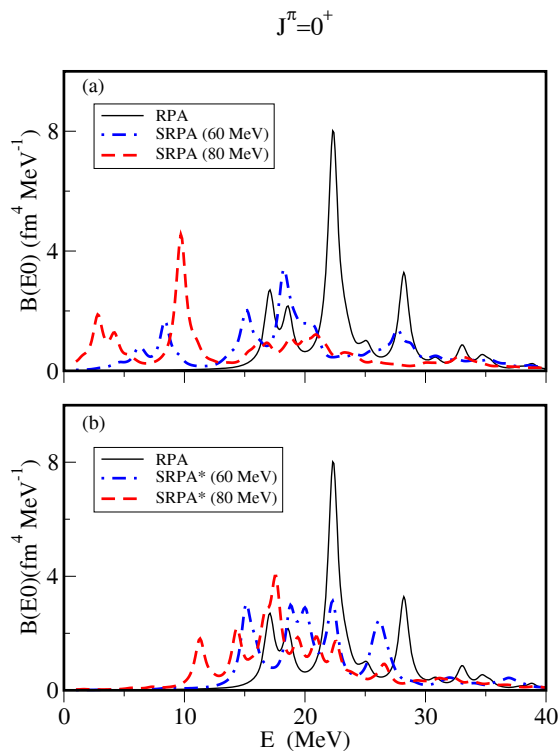


**Fig. 3.** (Color online) (a) Isoscalar monopole response calculated with the Gogny-RPA model (full line) and with the Gogny-SRPA approach with an energy cutoff on the  $2ph$  configurations of 60 (dotted line) and 80 (dashed line) MeV. (b) Same as in (a) but in the SRPA\* scheme. See the text for more details.

In the following we will indicate the two calculations a) and b) as SRPA and SRPA\*, respectively. The strong impact of the  $\nu\pi$  matrix elements of the interaction can be seen in fig. 3 where the isoscalar monopole response calculated in the SRPA (a) and in the SRPA\* (b) scheme is displayed for two values of the cutoff energy,  $E_{cut} = 60$  and 80 MeV. The corresponding Gogny-RPA results are also plotted in the two panels of the figure.

We see that in the SRPA scheme the responses associated with the different cutoff values are appreciably different and, for  $E_{cut} = 80$  MeV, the main peak of the response is pushed at energies more than 10 MeV lower than in the RPA case (a). The SRPA\* results of panel (b) are much more stable with respect to the change of the cutoff energy. This can also be seen by considering the centroid energies of the strength distributions. When the energy cutoff is increased from 60 to 80 MeV the centroid goes from 20.37 to 15.30 MeV (deviation of 25%) in the full SRPA calculations whereas it is much less shifted, from 23.97 to 22.37 MeV (7%), in the SRPA\* case. It is also worth noticing that in the latter case the difference between the spectra corresponding to the two energy cutoff is essentially just a shift, while when the  $\nu\pi$  matrix elements are not neglected, the SRPA strength distribution is very much different from the RPA one.

To check more in detail the stability of the results in the SRPA\* case, we have performed also calculations with

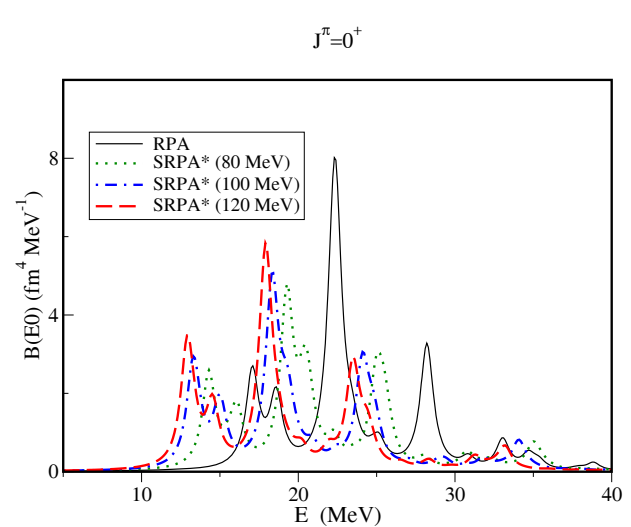


**Fig. 4.** (Color online) Gogny-SRPA\* isoscalar monopole response calculated with cutoff energies of 80 (dotted line), 100 (dot-dashed line) and 120 (dashed line) MeV. The Gogny-RPA results are also plotted for reference (full line).

cutoff values of 100 and 120 MeV (fig. 4). When the cutoff is changed from 80 to 100 MeV the centroid is shifted from 22.37 to 21.32 MeV (5%) and when the cutoff is changed from 100 to 120 MeV the centroid moves from 21.32 to 20.49 MeV (4%). On the contrary, the SRPA results still change significantly increasing the energy cutoff and for values larger than 80 MeV the solution of the corresponding equations is affected by the presence of a few imaginary eigenvalues. We conclude that the stability expected when the Gogny interaction is employed seems to be achieved in the SRPA\* case where, by construction, all the large  $\nu\pi$  matrix elements of the residual interaction in the beyond RPA blocks of the matrices are neglected.

## 4 Subtracted SRPA results

As shown and discussed in the previous section, we have seen that, independently of the kind of interaction adopted, the SRPA spectrum is systematically lowered by several MeV with respect to that obtained in the ordinary RPA. On the other hand, RPA results based on the EDF framework are typically in very good agreement with experimental data, at least concerning the centroid energies and total strength of the giant resonances. Ideally, when applied to the study of giant resonances, the SRPA should thus keep almost unchanged these quantities and provide a stronger fragmentation of the strength. As discussed in the introduction, very recently, a method to cure the too strong shift affecting in general all the beyond-RPA calculations, based on the so-called subtraction procedure has been proposed [11].

In this subsection we show the effect of this procedure on the SRPA results. We start considering the Skyrme-SRPA case. More details on the procedure and on the calculations can be found in [12]. Roughly speaking, the

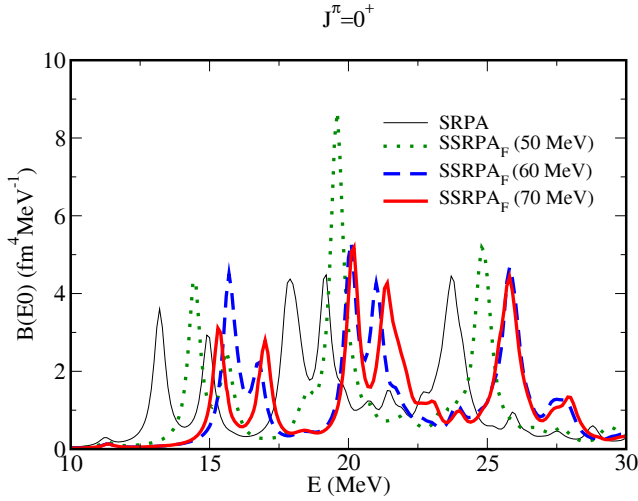


**Fig. 5.** (Color online) Isoscalar monopole response calculated in the standard Skyrme-SRPA (solid-thin line), and with the  $SSRPA_F$ , with a cutoff for the correction terms at 50 (dotted line), 60 (dashed line), and 70 (solid-thick line) MeV.

subtraction procedure consists in subtracting in the  $A_{11}$  block of the SRPA matrix the quantity

$$E_{11'} = - \sum_{2,2'} A_{12}(A_{22'})^{-1} A_{2'1'} - \sum_{2,2'} B_{12}(A_{22'})^{-1} B_{2'1'}, \quad (22)$$

guaranteeing that the “subtracted SRPA” response reduces to the RPA one in the zero-frequency limit. When density-dependent interactions are employed, the subtraction procedure is indeed more complex, modifying also the  $B_{11}$  matrix. More details can be found in ref. [12], where the full procedure adopted also in the present calculations has been described.

From a numerical point of view, the main cost in calculating the correction (22) consists in inverting the  $A_{22}$  matrix. This inversion becomes trivial if the matrix is assumed to be diagonal. Therefore the correction can be calculated with a reasonable extra-numerical effort. We use the acronyms  $SSRPA_F$  to denote the subtracted SRPA in the full scheme, *e.g.* full inversion of the  $A_{22}$  matrix, and  $SSRPA_D$  to denote the subtracted SRPA assuming diagonal the  $A_{22}$  matrix in the correction term (22). Therefore, for the  $2ph$  space in the SRPA calculations, we take the cutoff to be at 70 MeV. This value leads to about 5000  $2ph$  configurations in each of the two cases. This number is small enough so that we can still fully invert the matrix  $A_{22}$  to perform the subtraction.

Figure 5 shows the isoscalar monopole strength distribution, calculated with the unmodified SRPA and with the  $SSRPA_F$ , using a cutoff in the correction term equal to 50, 60, and 70 MeV. In the last of these cases, all the SRPA  $2ph$  configurations are included in the correction. The effect of the subtraction, as we expected, is to shift the SRPA spectrum upwards, by amounts that increase with the cutoff in the correction terms. The important differences between the three subtracted strength functions indicate that it is crucial to include all the  $2ph$  states in

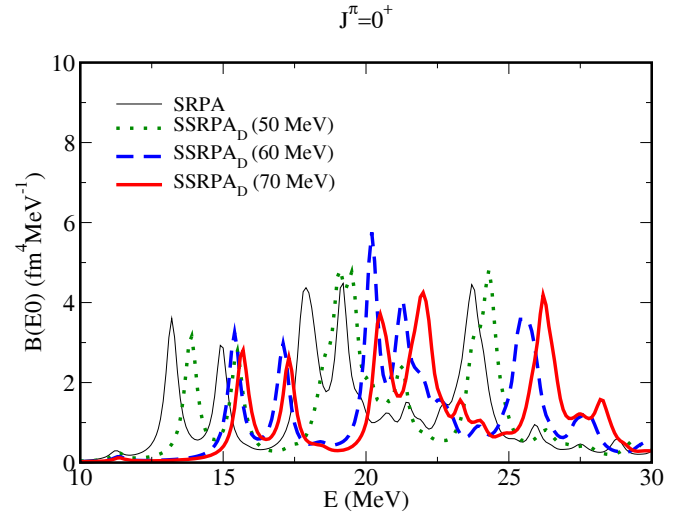


**Fig. 6.** (Color online) Same as in fig. 5, but in the diagonal approximation  $SSRPA_D$ .

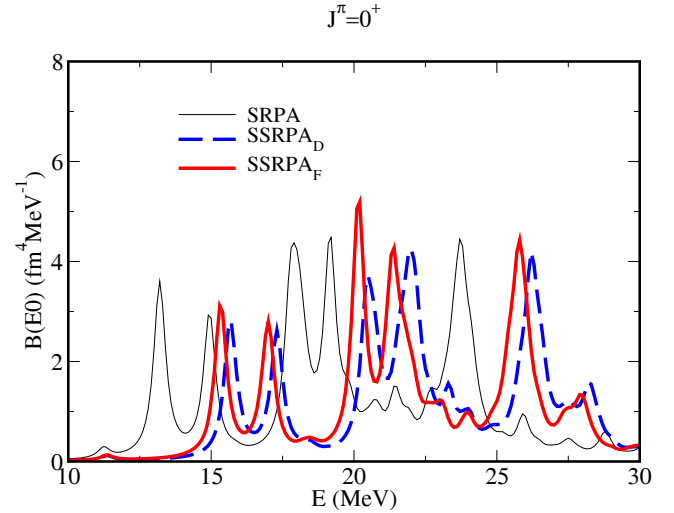


**Fig. 7.** (Color online) Isoscalar monopole response calculated in the Skyrme-SRPA without subtraction (solid-thin line), in the  $SRPA_D$  (dashed line) and in the  $SSRPA_F$  (solid-thick line), with a cutoff in the correction terms at 70 MeV.

the correction terms containing  $(A_{22'})^{-1}$  in eq. (22). The calculation must be coherent, that is, the  $2ph$  spaces used in the original SRPA matrices and in the correction terms should be the same.

Figure 6 shows the same results with the diagonal approximation  $SSRPA_D$  and fig. 7 compares the full and diagonal subtracted SRPA results with the 70 MeV cutoff in the correction terms. We observe that the  $SSRPA_F$  and  $SSRPA_D$  results are very similar, the difference being a small systematic shift to larger excitation energies in the  $SSRPA_D$ .

Another very positive feature of the  $SSRPA$  results is the very weakly dependence on the  $2ph$  cutoff. This can be seen in fig. 8, where we show the isoscalar monopole responses, with cutoffs for the correction terms at 70,

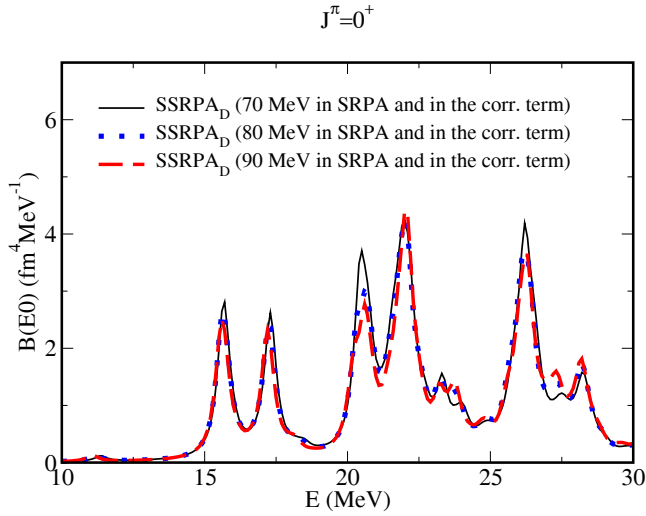


**Fig. 8.** (Color online) Isoscalar monopole response in the diagonal approximation Skyrme-SSRPA<sub>D</sub> with cutoff for the correction terms at 70 (full line), 80 (dashed line), and 90 (dotted line) MeV.

80, and 90 MeV. In each case, this cutoff is the same as that in the corresponding unsubtracted SRPA calculation. The three strength functions are very similar. We can see that the subtraction procedure not only rectifies the SRPA energy shifts for giant resonances, but also provides much more robust (cutoff-insensitive) results. We stress that a similar behavior has been found also for the isovector monopole and quadrupole responses. Moreover, the subtracted-SRPA approach improves significantly the agreement with the experimental data [12].

In the following, we will show the subtraction procedure applied to the Gogny-SRPA case. In this case, because of the finite range of the interaction, calculations are much heavier with respect to the Skyrme case. For this reason, in these first applications we calculated the correction (22) by using the diagonal approximation that has been found to be very reasonable in the Skyrme case. Further calculations to check this approximation also in the Gogny case are left for future studies. In fig. 9, the dependence on the cutoff on the  $2ph$  configurations included in calculating the correction (22) is studied in the SRPA and SRPA\* cases, in the upper and lower panels of the figure respectively. The subtracted results are indicated with SSRPA and SSRPA\*, corresponding to the case a) and b) discussed in see sect. 3.2 and we can see that the larger the cutoff is the bigger is the shift towards high energy provided by the subtraction procedure.

In fig. 10 the results obtained applying the subtraction method with the largest cutoff are compared with the SRPA and RPA results. One can see that, in both cases, the effect of the subtraction procedure is similar to the one observed in the previous cases when the Skyrme interaction was employed, producing a global shift upwards of the strength distributions. From panel (a) of the figure we can also see that the shift is stronger in the full SSRPA case, somehow curing the effect of those  $\nu\pi$  ma-

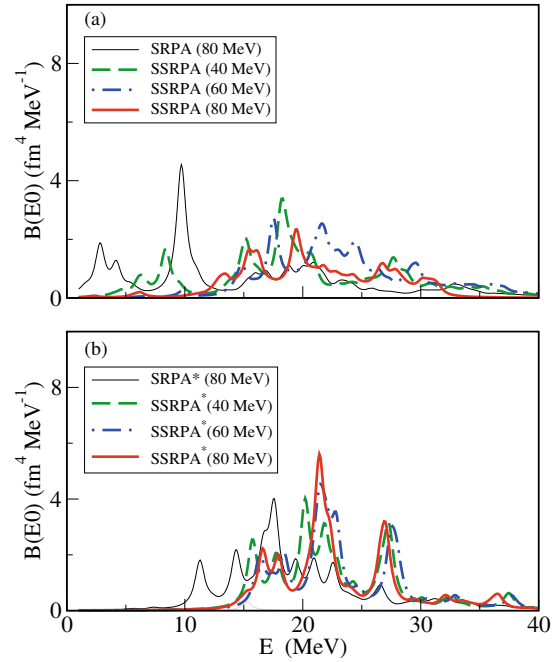


**Fig. 9.** (Color online) Dependence on the cutoff (value in parenthesis in MeV units) of the subtracted procedure in the Gogny case for the SSRPA and SSRPA\* in panel (a) and (b), respectively. The SRPA and SRPA\* with the largest cutoff are also shown for reference. The results refer to the isoscalar monopole case. See the text for more details.

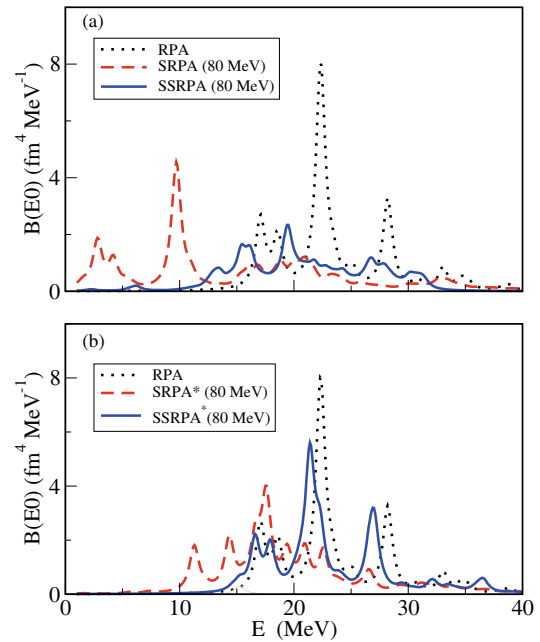


**Fig. 10.** (Color online) Panel (a): comparison between the Gogny-RPA, SRPA and SSRPA results; panel (b): same as panel (a) but for the SRPA\* and SSRPA\* cases. See the text for more details.

trix elements generating the very strong SRPA shift towards lower energy discussed before. However, the subtracted results in the two cases, still have significant dif-

ferences. For example the percentage of EWSR (integrate up to 40 MeV) and the corresponding centroid energy are 65% and 20.82 MeV in the SSRPA case, while 91% and 23.82 MeV in the SSRPA\* case. We checked that in both cases, the missing strength is located above 40 MeV as it is strongly fragmented over  $2ph$ -like excitations.

## 5 Conclusions

In this paper we have shown and discussed recent applications of the SRPA framework by using both the Skyrme and Gogny interactions. The SRPA scheme is fully treated without employing usually adopted approximations in the model space and in the evaluation of SRPA matrices. A general feature of the SRPA strength distributions for giant resonances is a several-MeV shift to lower energies with respect to RPA distributions.

When the Gogny interaction is employed, we have also found that the responses are very strongly affected by some  $\nu\pi$  matrix elements of the residual interaction, particularly in the channels which couple the  $1ph$  with the  $2ph$  configurations, *i.e.* 3 hole-1 particle type. These matrix elements do not contribute in Hartree-Fock and standard RPA calculations. Therefore, they do not contribute in the calculations where the parameters of the effective forces are fixed by the usual fitting procedures. To check and constrain their effects, it is thus necessary to go beyond the conventional procedures.

After that we have applied to the SRPA a subtraction procedure proposed by Tselyaev some years ago to overcome problems related to double counting in certain beyond-mean-field calculations. We have verified that the subtracted SRPA provides very robust predictions, which are stable and very weakly cutoff-dependent. Furthermore, the fulfillment of the stability condition, together with the elimination of double counting, substantially reduces the large anomalous shift downwards that the ordinary SRPA systematically produces with respect to the RPA strength. In particular, we also show the first applications where this procedure is applied to the Gogny-SRPA case. We show that this procedure is able to correct for the strong shift also when those anomalous proton-neutron matrix elements of the residual interaction mentioned before are included in the calculations.

Future and more systematic applications of the SS-RPA with both interactions are in order, for the study of giant resonances and low lying excitations, with particular emphasis in neutron rich systems.

## References

1. A. Bohr, B.R. Mottelson, *Nuclear Structure*, Vol. II (Benjamin Press, New York, 1975).
2. M.N. Harakeh, A. Van der Woude, *Giant Resonances* (Clarendon Press, Oxford, 2001).
3. P. Ring, P. Schuck, *The Nuclear Many-Body Problem* (Springer, New York, 1980).
4. D.J. Thouless, Nucl. Phys. **21**, 225 (1960).
5. P. Papakonstantinou, R. Roth, Phys. Lett. B **671**, 356 (2009).
6. P. Papakonstantinou, R. Roth, Phys. Rev. C **81**, 024317 (2010).
7. D. Gambacurta, M. Grasso, F. Catara, Phys. Rev. C **81**, 054312 (2010).
8. D. Gambacurta, M. Grasso, F. Catara, J. Phys. G **38**, 035103 (2011).
9. D. Gambacurta, M. Grasso, F. Catara, Phys. Rev. C **84**, 034301 (2011).
10. D. Gambacurta, M. Grasso, V. De Donno, G. Co, F. Catara, Phys. Rev. C **86**, 021304(R) (2012).
11. V.I. Tselyaev, Phys. Rev. C **88**, 054301 (2013).
12. D. Gambacurta, M. Grasso, J. Engel, Phys. Rev. C **92**, 034303 (2015).
13. P. Papakonstantinou, Phys. Rev. C **90**, 024305 (2014).
14. G. Lauritsch, P.G. Reinhard, Nucl. Phys. A **509**, 287 (1990).
15. K. Takayanagy, K. Shimizu, A. Arima, Nucl. Phys. A **477**, 205 (1988).
16. A. Mariano, F. Krmpotic, A.F.R. De Toledo Piza, Phys. Rev. C **49**, 2824 (1994).
17. D.J. Thouless, Nucl. Phys. **22**, 78 (1961).
18. D. Gambacurta, F. Catara, M. Grasso, M. Sambataro, M.V. Andrès, E.G. Lanza, Phys. Rev. C **93**, 024309 (2016).
19. V.I. Tselyaev, Phys. Rev. C **75**, 024306 (2007).
20. E.V. Litvinova, V.I. Tselyaev, Phys. Rev. C **75**, 054318 (2007).
21. E. Litvinova, P. Ring, V. Tselyaev, Phys. Rev. Lett. **105**, 022502 (2010).
22. T.H.R. Skyrme, Nucl. Phys. **9**, 615 (1959).
23. D. Vautherin, D. Brink, Phys. Rev. C **5**, 626 (1972).
24. J. Dechargé, D. Gogny, Phys. Rev. C **21**, 1568 (1980).
25. C. Yannouleas, Phys. Rev. C **35**, 1159 (1987).
26. S. Drozd, s. Nishizaki, J. Speth, J. Wambach, Phys. Rep. **197**, 1 (1990).
27. N. Van Giai, H. Sagawa, Phys. Lett. B **106**, 379 (1981).
28. D. Gambacurta, F. Catara, Phys. Rev. B **79**, 085403 (2009).
29. J. Dechargé, D. Gogny, Phys. Rev. C **21**, 1568 (1980).
30. J.F. Berger, M. Girod, D. Gogny, Comput. Phys. Commun. **63**, 365 (1991).